3

RESONANCE CURVES OF A SYNCHRONISED OSCILLATOR

B. R. NAG

INSTITUTE OF RADIO PHYSICS AND ELECTRONICS, CALCUTTA UNIVERSITY

(*Received for publication, September* 30, 1958)

ABSTRACT. Resonance curves of an oscillator with an external synchronising electromotive force capable of delineating the features of hysteresis effect have been determined experimentally with the help of a differential analyser. Theoretical resonance curves of an oscillator with a break-point non-linearity are deduced and compared with experimental curves. From the experimental curves the range of hysteresis is determined.

1. INTRODUCTION

Resonance curves of an oscillator with an external synchronising electromotive force have been studied both theoretically and experimentally by many workers (Appleton, 1922; Appleton and Van der Pol, 1922; Golz, 1922, Van der Pol, 1927, 1934; Andronov and Witt, 1930; Gapanov, 1935; Tucker, 1946; Cartwright, 1948; Gillies, 1949, 1954). However, the experimental measurements made by previous workers were only adequate to verify portions of the resonance curves obtained theoretically. Some important details of these theoretical curves have remained yet to be verified. For instance, it follows from theoretical analysis that the resonance curves of an oscillator obeying Van der Pol equation should show hysteresis over a range of synchronising voltages on the 'border line between strong and weak signals' (Cartwright, 1948), the exact range suggested by different authors being different. Nevertheless, as far as the present author is aware, the hysteresis effect has not been experimentally obtained by any worker. This is possibly due to the fact that the hysteresis occurs for values of parameters which are very close together and it is difficult to provide such close variation of the parameters in a determined way on an experimental oscillator. On a differential analyser, however, an oscillator may be easily realised of which the describing differential equation is definite and the parameters admit of accurate control. The resonance curves of the oscillator may thus be obtained with the help of a differential analyser in greater detail than is otherwise possible.

The work, described in the present paper, was first concerned with the Van der Pol oscillator and the experimental resonance curves were obtained on a differential analyser. Hysteresis effect was found to exist in these curves but the range was too small to be determined exactly. Moreover, a very accurate realisa-

tion of the cubic non-linearity of Van der Pol equation is difficult. The study was therefore extended to an oscillator which is stabilised by a break-point non-linearity, easily representable on the analyser and for which the range of hysteresis is wider. The theoretical resonance curves of this type of oscillator are not available and hence these have also been calculated.

2. THEORETICAL RESONANCE CURVES OF AN OSCILLATOR WITH AN EXTERNAL ELECTROMOTIVE FORCE

The differential equation describing an oscillator with an external electromotive force can be written as

$$\ddot{x}+\mu f(x, \dot{x})+\omega_0^2 x = E \sin \omega_1 t, \qquad (1)$$

where $\mu f(x, \dot{x})$ represents the non-linearity in the oscillator.

The solution of the above equation for small values of μ may be assumed to be given by

$$x = A \sin (\omega_1 t+\phi) \qquad \ldots (2)$$

where A and ϕ are functions of time.

Differentiating (2)

$$\dot{x} = \omega_1 A \cos (\omega_1 t+\phi)+\dot{A} \sin (\omega_1 t+\phi)+A\dot{\phi} \cos(\omega_1 t+\phi) \qquad \ldots (3)$$

Differentiating again and keeping only the first order terms (terms involving $\ddot{A}$, $\ddot{\phi}$ or $\dot{A}\ \dot{\phi}$ are neglected).

$$\ddot{x} = -\omega_1^2 A \sin (\omega_1 t+\phi)+2\omega_1 \dot{A} \cos (\omega_1 t+\phi)-2\omega_1 A\dot{\phi} \sin (\omega_1 t+\phi) \qquad \ldots (4)$$

Substituting for $\ddot{x}$, $\dot{x}$ and x in Eqn. (1) from Eqns. (4), (3) and (2) respectively and retaining the first order terms only

$$(\omega_0^2-\omega_1^2)A \sin (\omega_1 t+\phi)+2\omega_1 \dot{A} \cos (\omega_1 t+\phi)-2\omega_1 A\dot{\phi} \sin (\omega_1 t+\phi) = E \sin \omega_1 t-\mu f\{A \sin (\omega_1 t+\phi), \omega_1 A \cos (\omega_1 t+\phi)\}. \qquad \ldots (5)$$

Now, $\mu f\{A \sin (\omega_1 t+\phi), \omega_1 A \cos (\omega_1 t+\phi)\}$ may be written as

$$\mu f\{A \sin (\omega_1 t+\phi), \omega_1 A \cos (\omega_1 t+\phi)\} = g \cos (\omega_1 t+\phi)+h \sin (\omega_1 t+\phi) \qquad \ldots (6)$$

+ terms involving harmonics of ω_1.

where

$$g = \frac{1}{\pi} \int_0^{2\pi} \mu f\{A \sin(\omega_1 t+\phi), \omega_1 A \cos (\omega_1 t+\phi)\} \cos (\omega_1 t+\phi) d(\omega_1 t) \qquad \ldots (7)$$

and

$$h = \frac{1}{\pi} \int_0^{2\pi} \mu f\{A \sin (\omega_1 t+\phi), \omega_1 A \cos (\omega_1 t+\phi)\} \sin (\omega_1 t+\phi) d(\omega_1 t) \ldots \qquad (8)$$

Equating the co-efficients of $\cos(\omega_1 t+\phi)$ and $\sin(\omega_1 t+\phi)$ on the two sides of Eqn. (5)

$$\omega_1 \dot{A} = -\frac{1}{2} g - \frac{E}{2} \sin\phi. \qquad \ldots (9)$$

$$\omega_1 A \dot{\phi} = \frac{1}{2} h - \frac{A}{2}(\omega_1^2 - \omega_0^2) - \frac{E}{2} \cos\phi. \qquad \ldots (10)$$

For periodic oscillations, the equilibrium values of A and ϕ are obtained on putting $\dot{A} = 0, \dot{\phi} = 0$ in Eqns. (9) and (10).

Thus,

$$-g = E \sin\phi. \qquad \ldots (11)$$

$$h = A(\omega_1^2 - \omega_0^2) + E\cos\phi. \qquad \ldots (12)$$

On eliminating ϕ

$$E^2 = [h - (\omega_1^2 - \omega_0^2)A]^2 + g^2. \qquad \ldots (13)$$

Eqn. (13) gives the amplitudes of periodic oscillations for different excitations and detuning The plots of A^2 or normalised values of A^2 against $\frac{\omega_1^2 - \omega_0^2}{\omega_1}$ are referred to as the resonance curves of the oscillator.

Resonance Curves of the Van der Pol Oscillator

For the Van der Pol oscillator,

$$\mu f(x, \dot{x}) = c\dot{x}^3 - a\dot{x}. \qquad \ldots (14)$$

Hence

$$g = \left(\frac{3}{4} c\omega_1^2 A^2 - a\right) \omega_1 A. \qquad \ldots (15a)$$

$$h = 0 \qquad \ldots (15b)$$

On substituting in Eqn. (13)

$$E^2 = [(\omega_1^2 - \omega_0^2)A]^2 + \left[\left(\frac{3}{4} c\omega_1^2 A^2 - a\right) \omega_1 A\right]^2 \qquad \ldots (16)$$

Putting $\frac{4a}{3c} = A_0^2$, $\frac{\omega_1}{A_0} A = \rho$, $\frac{\omega_1^2 - \omega_0^2}{\omega_1 a} = \sigma$, $\frac{E}{aA_0} = F$

$$F^2 = \rho^2[\sigma^2 + (1 - \rho^2)^2] \qquad \ldots (17)$$

In the resonance curves shown in figure 1, ρ^2 is plotted against σ with F^2 as parameter. Since the plots are symmetrical about σ, the portions for positive values of σ are only shown.

It is observed that for low values of F^2, the resonance curves have two branches and there are three values of ρ^2 for low values of σ. With increase in F^2, the two branches approach each other and meet on the $\sigma = 0$ axis for $F^2 = \frac{4}{27}$; with further increase in F^2 the curve opens out but continues to have triple value of ρ^2 for some values of σ till $F^2 = \frac{5}{27}$. For larger values of F^2 the resonance curves are single-valued.

The equilibrium values of ρ^2 as given by Eqn. (17) are not all necessarily stable. The stability can be judged on considering the singularities of the first order differential equation, (Andronov and Witt, 1930) which may be derived, from Eqns (9) and (10) as

$$\frac{d\rho}{d\phi} = \rho \frac{-(\rho^2 - 1)\rho - F\sin\phi}{-\sigma\rho - F\cos\phi} \qquad \ldots \quad (18)$$

The singularities of this equation are of the form shown in figure 1. The equations for the critical lines are given by

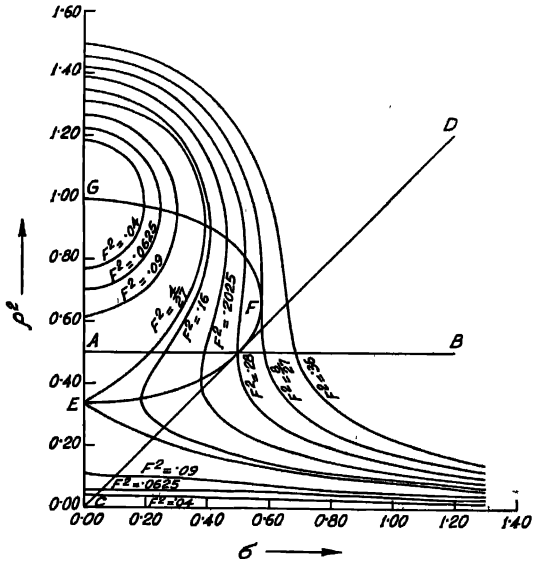

Fig. 1(a). Theoretical resonance curves of Van der Pol oscillator.

(i) $\rho^2 = \frac{1}{2}$ (line A B)

(ii) $\rho^2 = \sigma$ (line C D)

(iii) $\sigma^2 = -(1-\rho^2)(1-3\rho^2)$ (Curve E F G).

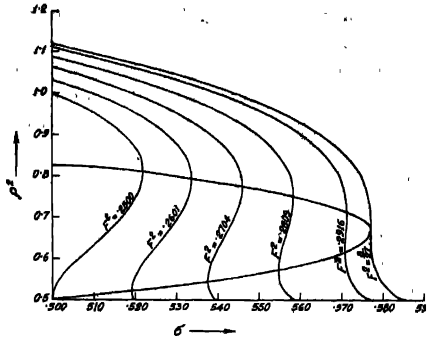

Fig. 1(b) Theoretical resonance curves of Van der Pol oscillator showing the region of hysteresis.

Evidently in the regions where the singularities are of the nature of saddles, unstable nodes or unstable spirals, the values of ρ^2 given by the resonance curves represent unstable equilibrium. Now, when a periodic solution becomes unstable, the oscillator will execute the other stable periodic oscillation, if there be any in the region. In regions where no periodic stable oscillation is possible, the oscillator will execute the other possible oscillation which has been called the quasi-periodic oscillation In that case $\dot{A}$ and $\dot{\phi}$ do not become zero but vary periodically giving rise to a limit cycle in the $A-\phi$ plane.

On the basis of the above considerations, the transformation from periodic to quasi-periodic oscillation or vice versa can be readily predicted. The $\rho^2-\sigma$ plane can be divided into three regions characterised by the different ways in which the transformation from periodic to quasi-periodic oscillation or vice versa takes place.

(i) *Region extending from* $F^2 = 8/27$ *upwards* : For such values of F^2, the periodic oscillation becomes unstable on AB. Hence as σ is varied from lower to higher values the periodic oscillation continues following the resonance curve till it reaches the line AB. Quasi-periodic oscillations will thereafter be excited, i.e., a limit cycle will appear round the unstable focus which will continue for higher values of σ; the r.m.s. value of the amplitude will gradually increase to the free oscillation value. The curves will be reversible.

(ii) *Region extending from* $F^2 = 4/27$ *downwards* : In this case the transformation will take place on the upper part of the curve $E\,F\,G$; the limit cycle will transform to a separatrix through the double singularity. The resonance curves again will be reversible.

(iii) *Region extending from* $F^2 = 4/27$ *to* $F^2 = 8/27$: The transformation from periodic to quasi-periodic oscillation or vice versa cannot be so readily

predicted in this case. For values of $F^2 \geqslant 9/32$, for which the resonance curves cut the upper part of the curve EFG at a lower value of σ than that for the lower part, the limit cycle is expected to penetrate the curve EFG and transformation will take place on AB. The response curve will show hysteresis. As σ is decreased the r m.s. amplitude of quasi-periodic oscillation will gradually decrease and the oscillation transforms to periodic oscillation on AB. With further decrease in σ, the amplitude will follow the resonance curve till it cuts the lower part of EFG. At this point it will jump to the higher stable value. For further reduction of σ it will again follow the resonance curve. When σ is increased from lower to higher values the amplitude of oscillation follows the resonance curve till it meets the upper part of EFG. At this point the amplitude jumps to the lower stable value. It will be seen that this downward jump occurs for a value of σ higher than that for which the upward jump occurs for the reverse variation of σ.

For values of F^2 lower than 9/32, however, the transformation can not be definitely predicted The point of transformation may shift suddenly from AB to the upper part of EFG for $F^2 < 9/32$. In that case the hysteresis effect will be exhibited only in the periodic oscillations. The range of hysteresis will extend from $F^2 = 9/32$ to $F^2 = 8/27$ (Gapanov, 1935). It has been suggested by Cartwright (1948) that this discontinuous behaviour on the two sides of $F^2 = 9/32$ is improbable and that the quasi-periodic oscillation will continue to transform to periodic oscillation on AB upto $F^2 = 1/4$ as in the above case Then the transformation point will gradually move up i.e, the limit cycle instead of vanishing through a focus will vanish through a saddle point. However, this transformation point will move up to the upper part of EFG before $F^2 = 4/27$ If this suggestion is correct, the response curve will show jumps from lower periodic oscillations to upper periodic oscillations in the region $1/4 \leqslant F^2 \leqslant 9/32$ and from lower quasi-periodic to upper periodic oscillation in the region $4/27 \leqslant F^2 \leqslant 1/4$ The downward jumps will be from upper periodic oscillation to lower quasi-periodic oscillation. The region of hysteresis will extend from $F^2 = 4/27 + \delta$ to $F^2 = 8/27$, δ being an undetermined positive number.

Alternatively it has been suggested by Gillies (1954) that the transformation will continue to take place on the upper part of the curve EFG even for $F^2 > 1/4$. But in between $F^2 = 1/4$ and $F^2 = 9/32$, there will be some value of F^2 for which the limit cycle passes through a second order singularity on the upper part of EFG, but instead of degenerating to a separatix when the singular points separate, a new limit cycle will appear which will continue to exist shrinking up round the unstable focus to vanish on AB. For larger values of F^2 the second order singularity appears outside the limit cycle and the latter therefore will continue to exist upto AB when it vanishes to a focus. Accordingly hysteresis should extend from $F^2 = 1/4 + \delta$ to $F^2 = 8/27$. Numerical integrations performed by Gillies seem to indicate that $\delta > 1/108$.

It is difficult to ascertain which one of the above suggestions is correct. A proper experimental determination of the range of hysteresis is also not easy in this case, since the range is very small. For example, for $a = 0.1$, $A_0 = 1$ the hysteresis range for E^2 as given by the three solutions are (1) .053—.0545, (Gapanov), (2) .050—δ—.0545 (Cartwright), (3) .050+δ—.0545 (Gillies). Thus a decision can be reached only when the experimental accuracy is of the order of 1 in 1000; this is difficult to be attained on an electronic differential analyser.

Resonance Curves of an Oscillator Stabilised by Break-point Non-linearity

We next consider an oscillator for which

$$\mu f(x, \dot{x}) = f_1(\dot{x}) - a\dot{x}$$

$$f_1(\dot{x}) = \dot{x} - E_0, \quad \text{for} \quad \dot{x} > E_0$$

$$= 0, \quad \text{for} \quad -E_0 < \dot{x} < E_0$$

$$= \dot{x} + E_0, \quad \text{for} \quad -E_0 > \dot{x}$$

This non-linearity has been called the break-point non-linearity and is shown graphically in figure 2. It may be mentioned that the operating conditions of a

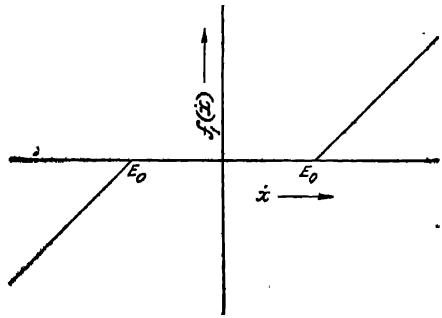

Fig. 2. The break-point non-linearity.

practical oscillator are such that this type of non-linearity is nearer to the actual conditions than the cubic non-linearity.

In this case, from Eqns. (7) and (8),

$$-g = \omega_1 A \left[a - \frac{2}{\pi} \cos^{-1} \frac{E_0}{\omega_1 A} + \frac{2}{\pi} \left(\frac{E_0}{\omega_1 A} \right) \sqrt{1 - \left(\frac{E_0}{\omega_1 A} \right)^2} \right], \text{ for } \omega_1 A > E_0$$

$$= \omega_1 A a, \quad \text{for} \quad \omega_1 A < E_0$$

$$k = 0 \qquad \ldots \quad (18)$$

Substituting these values of g and h in Eqn. (13) and putting

$$\frac{\omega_1 A}{E_0} = \rho_b, \quad \frac{\omega_1^2 - \omega_0^2}{\omega_1} = \sigma_b, \quad \frac{E}{E_0} = e$$

$$\left.\begin{aligned} \frac{e^2}{\rho_b^2} &= \left[a - \frac{2}{\pi} \cos^{-1}\frac{1}{\rho_b} + \frac{2}{\pi}\frac{1}{\rho_b}\sqrt{1-\frac{1}{\rho_b^2}}\right]^2 + \sigma_b^2, \text{ for } \rho_b > 1 \\ &= a^2 + \sigma_b^2, \quad \text{for} \quad \rho_b < 1 \end{aligned}\right\} \quad \ldots (19)$$

In contrast to the previous case normalised (with respect to a) plots of the resonance curves cannot be given. Plots for the particular value of $a = 0.1$ are shown in figure 3.

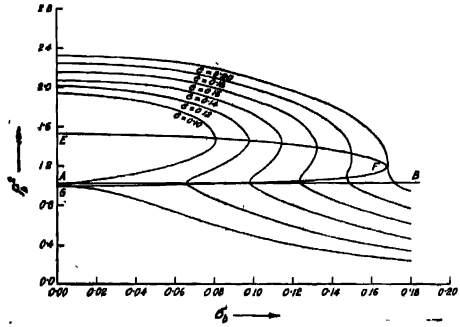

Fig. 3(a). Theoretical resonance curves of an oscillator with break-point non-linearity.

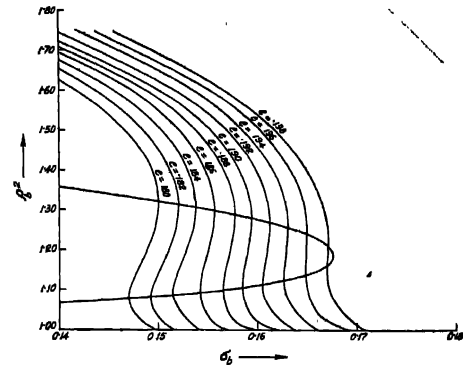

Fig. 3(b). Theoretical resonance curves of an oscillator with break-point non-linearity showing the region of hysteresis.

The general characteristics of the curves are similar to those of figure. 1. For $e < 0.1$, there are three values of ρ_b for low values of σ_b, while for $e > 0.198$ there is only one value of ρ_b for any value of σ_b. For intermediate values of e there are three values of ρ_b for some intermediate values of σ_b.

The equations for the critical lines separating the $\rho_b{}^2-\sigma_b$ plane into different regions characterised by different types of singularities are

$$\text{(i)} \quad \frac{1}{\rho_b} = \cos\frac{\pi}{2}a. \qquad \text{(line } AB\text{)}$$

$$\text{(ii)} \quad \frac{1}{\rho_b}\left(1-\frac{1}{\rho_b{}^2}\right)^{1/2} = \frac{\pi}{2}\sigma_b. \quad \text{(curve } CD\text{)}$$

$$\text{(iii)} \quad \sigma_b{}^2 = -\left(a-\frac{2}{\pi}\cos^{-1}\rho_b{}^{-1}\right)^2 + \left(\frac{2}{\pi}\frac{1}{\rho_b}\sqrt{1-\frac{1}{\rho_b{}^2}}\right)^2$$

(Curve EFG)

The reversible transformations from periodic to quasi-periodic oscillation or vice versa on the upper part of EFG occur for $e < 0.139$ and on AB for $e > 0.1985$. The range of hysteresis according to Cartwright's solution should extend from $e = 0.139-\delta$ to $e = 0.1985$; according to that of Gillies from $= 0.139+\delta$ to $e = 0.1958$; and according to that of Gapanov from $e = 0.184$ to $e=0.1985$. It is observed that the range of hysteresis for this oscillator is wider than in the case of the van der Pol oscillator for the same value of initial damping ($a = 0.1$). The study of the resonance curves of this oscillator is thus expected to yield more definite results.

3. EXPERIMENTAL ARRANGEMENT

The set up of the differential analyser for solving Eqn. (1) is shown in figure 4. The solution x appears at A and $\dot{x}$ at B. The sinusoidal synchronising voltage

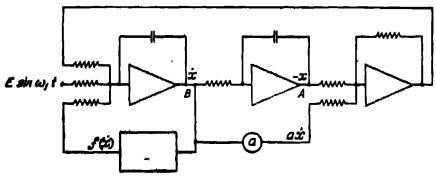

Fig. 4. Set up of the differential analyser for solving the equation;

$$\ddot{x}+f(\dot{x})-ax+\omega_0{}^2\,x = E\sin\omega_1\,t.$$

is supplied by an oscillator, stabilised by biased diodes, set on the analyser. Different values of σ are set by adjusting the frequency of the synchronising voltage which can be varied accurately by amounts as small as 0.01 per cent. The mean square amplitude of $\dot{x}$ is measured by a thermocouple in conjunction

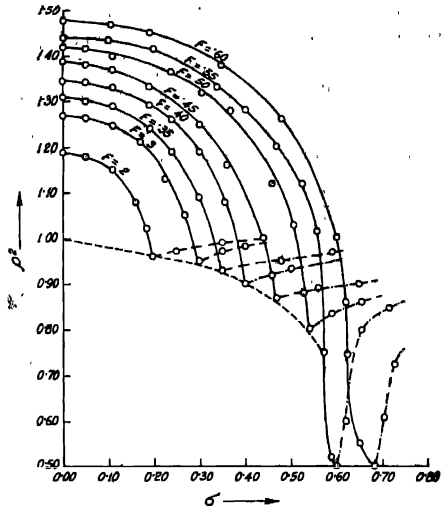

Fig. 5(a). Experimental resonance curves of Van der Pol oscillator.

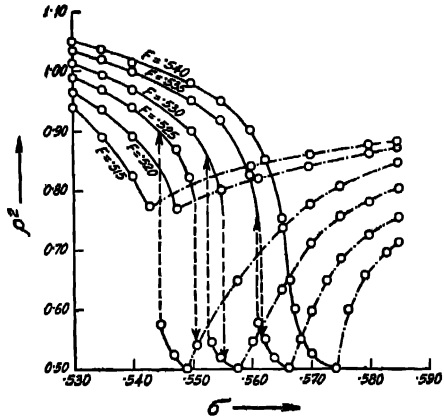

Fig. 5(b). Experimental resonance curves of Van der Pol oscillator showing the region of hysteresis.

with a d.c. millivoltmeter. The oscillator frequency is so chosen that the thermal inertia of the heater element of the thermocouple is large enough to give the average value. It may be noted that the accuracy of the differential analyser as obtained by test solutions is better than 1%.

4. EXPERIMENTAL RESULTS

The experimental plots of the resonance curves of the van der Pol oscillator are shown in Figure 5 and those for the oscillator with break-point non-linearity for $a = 0.1$ in figure 6.

Figures. 5(a) and 6(a) indicate very close qualitative agreement between the experimental and the theoretical curves. The reversible transformations from periodic to quasi-periodic oscillation or vice versa on the upper part of the curves EFG for low values of F and e and on the line AB for high values of F and e are clearly shown

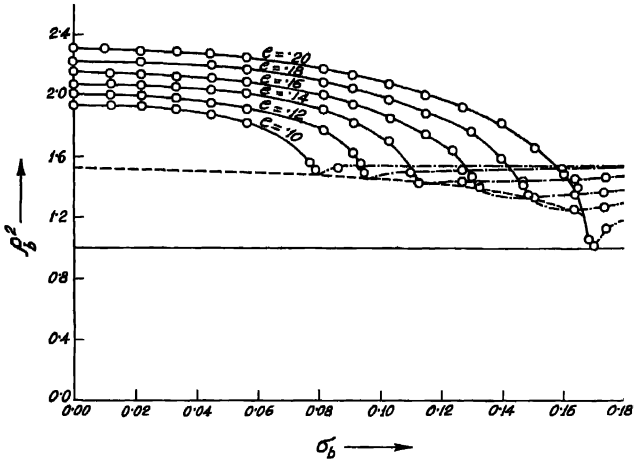

Fig. 6(a). Experimental resonance curves of an oscillator with break-point non linearity.

The detailed resonance curves shown in figures 5(b) and 6(b) show that hysteresis effect occurs in both the cases. The range of hysteresis of Van der Pol oscillator being comparatively narrow, detailed examination of the resonance curves in the hysteresis region is almost ruled out. But the curves for the oscillator with break-point non-linearity show all the details expected theoretically. The jump from low values of periodic oscillation to high values or vice versa is shown within the range $0.184 \leqslant e \leqslant 0.194$. It is further observed that hysteresis is obtained upto $e = 0.180$. In the region $0.180 \leqslant e \leqslant 0.184$, the upward jump continues to be from low periodic to high periodic oscillation, while the downward jump occurs from high periodic to low quasi-periodic oscillation. Jump from low quasi-periodic oscillation to high periodic oscillation as suggested by Cartwright has not been observed. The range of hysteresis extends from 0.196 to values of

e definitely greater than 0.178 and less than 0.184 and agrees more closely with Gillies's solution. However, the mechanism of shift of the transformation point from the line AB to the upper part of EFG appears to be different. Previous theoretical analyses indicated that with decrease in σ_b, the limit cycle should always shrink. Experimental curves show, however, that for $e > 0.198$ the limit cycles shrink with decrease in σ_b to vanish through a focus. But for values of $e < 0.180$ the limit cycle at first shrinks and then expands to vanish through a separatrix on the upper part of EFG.

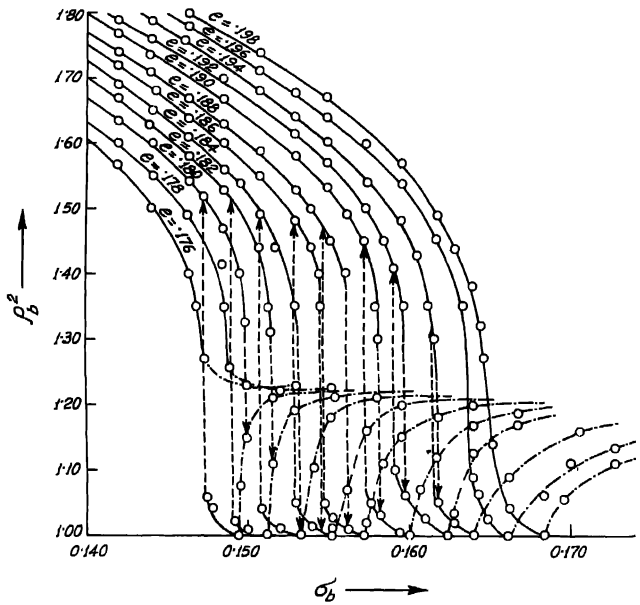

Fig. 6(b). Experimental resonance curves of an oscillator with break-point non-linearity showing the region of hysteresis

5. CONCLUSION

The experimental resonance curves obtained by a differential analyser agree very closely with the theoretical curves obtained by Van der Pol's method. The hysteresis phenomenon is clearly shown by the experimental curves. The range of hysteresis is found to be in good accord with the solution due to Gillies. In the oscillator with break-point non-linearity, the quasi-periodic oscillation in the border region shows a minima in amplitudes.

ACKNOWLEDGMENT

The author is indebted to Professor J. N. Bhar, D.Sc., F.N.I., for his constant guidance during the progress of the work.

REFERENCES

Appleton, E. V , 1922, *Proc. Cambr. Phil. Soc.*, **21**, 231.

Appleton, E. V. and Van der Pol, B., 1922, *Phil. Mag* , **43**, 189.

Andronov, A and Witt, A , 1930, *Archiv fur Electrotechnik*, **24**, 99.

Cartwright, M L., 1948, *J.I.E.E.*, Part III, **95**, 88.

Gapanov, W. I , 1935, *Journal of Technical Physics*, **5**, 821.

Golz, J., 1922, Jahrbuch der drahtlosen Telegraphie and Telephonie, **19**, 281.

Gillies, A W , 1949, *Proc. I.E.E.*, Part III, **96**, 453.

Gillies, A. W., 1954, *Quart. Jour. Mecha. Appl. Math.* Part II, **7**, 152.

Kryloff, N. and Bogoliuboff, N., 1949, 'Introduction to Non-linear Mechanics', Princeton University Press, Pp 79-87.

Minorsky, N., 1947, 'Introduction to Non-linear Mechanics', Edwards Brothers, Inc., Pp. 341-354.

Tucker, D. G., 1946, *J.I.E E.*, Part III, **92**, 226.

Van der Pol, B., 1927, *Phil. Mag.*, **3**, 65

Van der Pol, B., 1934, *Proc. I.R E.*, **22**, 1051.